Crystallization, Melting, and Morphology of Syndiotactic Polypropylene Fractions. 3. Lamellar Single Crystals and Chain Folding

Zhengzheng Bu, Yeocheol Yoon, Rong-Ming Ho, Wensheng Zhou, Ittipol Jangchud, R. K. Eby, and Stephen Z. D. Cheng*

Maurice Morton Institute and Department of Polymer Science, The University of Akron, Akron, Ohio 44325-3909

Eric T. Hsieh, Tim W. Johnson, Rolf G. Geerts, Syriac J. Palackal, Gil R. Hawley, and M. Bruce Welch

Research and Development, Phillips Petroleum Company, Bartlesville, Oklahoma 74004

Received March 12, 1996; Revised Manuscript Received June 26, 1996[⊗]

ABSTRACT: Highly faceted, regular, lathlike lamellar single crystals of syndiotactic polypropylene (s-PP) fractions have been investigated through transmission electron microscopy (TEM), atomic force microscopy (AFM), and electron diffraction (ED). Single crystals of s-PP over 1 μm in size can be grown from the melt in thin films. ED results obtained from the s-PP single crystals indicate a unit cell III with $a = 1.450$ nm, $b = 1.120$ nm, and $c = 0.740$ nm as proposed by Lovinger and Lotz. At high crystallization temperatures, relatively low molecular weight s-PP fractions can grow lamellar single crystals with microsectors. The polyethylene decoration method has been used to identify the chain folding direction, and no preferred orientation has been observed on the nonsectorized lamellar crystals. Sectorized lamellar single crystals show two different regions. In the sectors along the long axis (the *b*-axis), the chain folding is found to be parallel to the 010 direction. In the sectors along the short axis (the *a*-axis), little preferred orientation can be found. The deformation method of nonsectorized, high molecular weight s-PP single crystals on a plastic film has also been utilized to determine the chain folding direction. Microfibrillar structures can be observed in the cracks of the single crystals along both the *a*- and *b*-axes after deformation. This indicates that the folding direction in these nonsectorized, high molecular weight s-PP single crystals may be either along the (110) planes or a combination of the (100) and (010) microfolding and microsectoring. Zigzag-shaped edges on the deformed single crystals along the *a*-axis are also observed, and the sliding planes can be identified as the (110) planes.

Introduction

Syndiotactic polypropylene (s-PP) exhibits polymorphism due to different chain conformations and packing schemes. The high-temperature orthorhombic form in s-PP crystals is thermodynamically the most stable crystal form. The chain has an s(2/1)2 symmetry corresponding to a $(t_2g_2)_2$ conformation. Its crystal unit cell was first determined by Natta *et al.* through wide-angle X-ray diffraction (WAXD) fiber patterns.[1] The unit cell parameters were initially proposed to be *C*-centered orthorhombic[1] with $a = 1.450$ nm, $b = 0.580$ nm (later, it was found that $b = 0.560$ nm),[2] c (chain axis) $= 0.740$ nm, and $\alpha = \beta = \gamma = 90°$ with a $C222_1$ space group. The determination of this symmetry was based on the systematic absence of $h + k = 2n + 1$ reflections in the WAXD fiber patterns.

Lotz, Lovinger, *et al.* in the late 1980s observed reflections and streaks through electron diffraction (ED) of lamellar single crystals in s-PP thin films which were different from the expected ED reflections based on the $C222_1$ space group.[3−6] The presence of $h + k = 2n + 1$ reflections, which had not been seen in the fiber patterns and are forbidden for a unit cell with a space group of $C222_1$, were clearly identified. As a consequence, the introduction of a new unit cell (cell II) having different symmetry was necessary. This unit cell should have the same dimensions as unit cell I, but with helices of alternating handedness incorporated along the *a*-axis, resulting in a unit cell face-centered on the *ac* plane with a space group $Pca2_1$. Furthermore, based on the ED reflections in single crystals isothermally crystallized at high temperatures, an orthorhombic unit cell (cell III) has been proposed with $a = 1.450$ nm, $b = 1.120$ nm, $c = 0.740$ nm, and a space group of *Ibca*. The unit cell II is then recognized as a subcell of unit cell III. The "doubling" of the original unit cell I along the *b*-axis is a consequence of the different chain packing. Incorporation of both left- and right-handed helices is allowed in the lattice along both the *a*- and *b*-axes (antichiral packing).[3−6] Existence of the separate unit cell I has still been found by De Rosa and Corradini via their study of annealed s-PP WAXD fiber patterns.[7] Besides the high-temperature orthorhombic form, a low-temperature orthorhombic form and a triclinic cell have also been reported recently.[8,9]

The s-PP crystal morphology has not been given much attention in the past 30 years. One publication by Marchetti and Martuscelli[10] for solution-grown single crystals in various solvents appeared in 1974. The morphology of melt-crystallized lamellar single crystals and spherulitic textures in thin films and its dependence on undercooling were first reported by Lovinger *et al.* in 1991.[5] Their samples possessed a racemic diad content of 0.769 and syndiotactic and isotactic triad contents of 0.698 and 0.159, respectively. At the lowest undercoolings (the highest crystallization temperatures of $T_c > 105$ °C), large, rectangular and faceted lamellar crystals were observed by phase-contrast light microscopy and transmission electron microscopy (TEM). Based on the ED patterns, these crystals have the same

* To whom correspondence should be addressed.

[⊗] Abstract published in *Advance ACS Abstracts,* September 1, 1996.

S0024-9297(96)00379-8 CCC: $12.00

Table 1. Molecular Characterization of s-PP Fractions

sample	M_n ($\times 10^{-3}$)	M_w ($\times 10^{-3}$)	M_w/M_n	[r] (%)[a]	[rr] (%)[b]	[rrrr] (%)[c]	r-block[d]
s-PP(5)	33.3	36.6	1.1	94	92	86	34.1
s-PP(9)	132.0	158.4	1.2	95	92	87	33.9

[a] Racemic conformation [r]. [b] Triads [rr]. [c] Pentads [rrrr]. [d] Number-averaged syndiotactic block, 2([rr] + [mr]/2)/[mr].

unit cell and interchain packing as cell III. At a high undercooling (a T_c of 90 °C), twinned crystals seem to be more common. As T_c was decreased, the morphology became axialitic and eventually spherulitic (T_c around 60 °C). ED patterns with increasing streaking along the *h*20 reflections (cell III) suggested that with increasing undercooling, the intermolecular packing along the *a*-axis systematically deviates from the regular antichiral form due to kinetic factors during crystallization. Specifically, the packing disorder, as described previously, was believed to be introduced along the *b*-axis with the incorporation of isochiral chains. More recently, the crystal morphology of s-PP with high syndiotacticity has also been studied.[11] The essential features reported in ref 5 are not changed except for the shift of crystallization temperature, which is due to the higher melting temperatures observed. Along this line of research, overall crystallization, linear crystal growth, and melting behaviors have been investigated.[12,13] Lovinger *et al*. have also reported that the chain folding direction of s-PP single crystals grown at high temperature is along the *b*-axis based on their polyethylene (PE) decoration method.[11]

In this publication, we attempt to study the detailed morphology of the s-PP lamellar single crystals via TEM, atomic force microscopy (AFM), and ED. Both sectorized and nonsectorized s-PP lamellar single crystals can be observed. The chain folding behavior of these single crystals has been investigated using both PE decoration[14,15] and single-crystal deformation on the plastic films.[16,17]

Experimental Section

Materials and Samples. The s-PP fractions used in this study were kindly supplied by Phillips Petroleum Co. (Bartlesville, OK). A detailed molecular analysis was reported in the first part of this series.[12] Two of these s-PP fractions were studied to examine the molecular weight effect. Their molecular characteristics are listed in Table 1. Thin-film samples were prepared for TEM, AFM, and ED experiments. They were obtained via a solution-cast method and had a thickness of ~0.05−0.1 μm. When the single-crystal deformation method was applied, the s-PP samples were crystallized on Mylar films.

Instrumentation and Experiments. Crystal morphology was observed via TEM (JEOL JEM-1200IIX) with an accelerating voltage of 120 kV. The thin films were also isothermally crystallized at different temperatures by heating the samples to 180 °C and held isothermally for 2 min in one hot stage (Mettler FP-80HT). They were then quickly switched to another hot stage (Mettler FP-84HT) which was preset at an isothermal temperature. After complete crystallization, the films were cooled to room temperature. The film samples were then subjected to conventional Pt−C shadowing and carbon backing before being transferred to copper grids.

For the polymer decoration experiments,[14,15] a linear PE fraction with a weight-average molecular weight of 11 000 was used. The polydispersity of this fraction was 1.1. A small amount of PE powder was placed in a wire basket in a vaporizer. A 10 cm distance between the sample and the basket in the vacuum evaporator was chosen to avoid possible surface melting of the s-PP single crystals. On the other hand, for the lamellar single crystals, s-PP single crystals were grown on Mylar strips having a width of about $^1/_8$ in., and the films were uniformly drawn to various degrees ranging from nominal strain values of 5% to 30% on a small tensiometer.

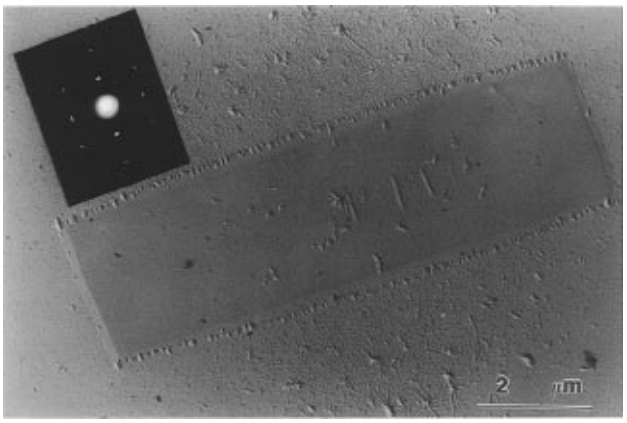

Figure 1. s-PP lamellar single crystals crystallized at 125 °C observed under TEM (M_n = 33.3K).

ED experiments were also carried out in the same TEM. Calibration of the ED spacing was carried out using Au and TlCl in a *d*-spacing range smaller than 0.384 nm, which is the largest spacing for TlCl. Spacing values greater than 0.384 nm were calibrated by doubling the *d*-spacing of those reflections based on their first-order reflections.

AFM (TopoMetrix TMX 2000) was used to examine the surface topology of the s-PP single crystals at ambient conditions. A 70 μm scanner was selected to fully cover the single crystal, and standard pyramid-shaped tips were chosen. Two AFM operation modes, the constant-force mode and the variable-force mode, were employed for sample scanning, but only constant-force images were used in the quantitative thickness study. The force used at the cantilever was set as light as possible to reduce damage to the sample, but heavy enough so that the surface features could be accurately scanned (~1−5 nN). The scanning rate was controlled to be 1−3 Hz for the low-magnification images. Resolutions of 300 × 300 and 500 × 500 data points per image were used to collect the data. Lamellar thicknesses were obtained through scans across the single crystals.

Results and Discussion

Lamellar Single Crystals. Figure 1 shows a highly faceted, regular, lath-shaped lamellar single crystal grown at 125 °C from the melt. ED pattern is also included with proper crystallographic orientation. The single-layer lamella shows a smooth fold (top) surface and has an elongated *b*-axis. A similar shaped lamellar single crystal grown at 130 °C is shown in Figure 2 and the ED pattern is also included. Note that both crystals in Figures 1 and 2 were grown using a s-PP fraction of M_n = 33 300. One may use the concept of aspect ratios to describe the morphology of these single crystals. The aspect ratio is the ratio between the length along the *b*-axis and that of the *a*-axis. The aspect ratio values of these two crystals are 3.6 and 8.6, respectively. This indicates that the crystal growth along these 100 and 010 directions is highly anisotropic in the s-PP lamellar single crystals.

In Figure 2, it is surprising to see that microsectors can be clearly observed on the top surface of the single crystal. Two sector lines are found along the diagonal directions of the regular single crystal, dividing the

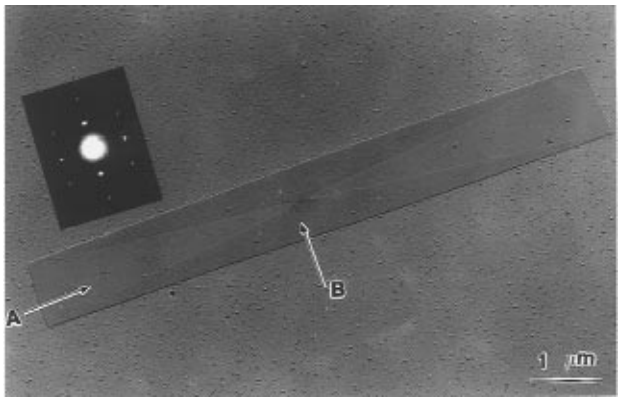

Figure 2. s-PP lamellar single crystals having sectorization crystallized at 130 °C observed under TEM (M_n = 33.3K).

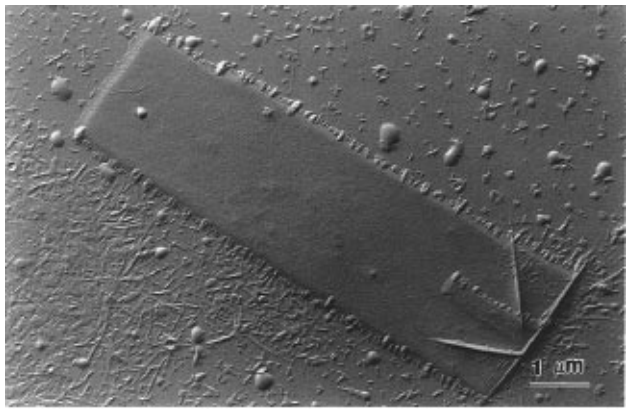

Figure 3. s-PP lamellar single crystals crystallized at 130 °C observed under TEM (M_n = 132.0K).

crystal into four sectors. These four surface sectors, also called surface domains, are in twin relationship to each other. This sectorization phenomenon is totally different from that observed in s-PP single crystals from solution crystallization.[10] In the latter case, the sector line was observed along the longitudinal direction of the elongated single crystal and divided the crystal into two sectors. Therefore, the sectorization in Figure 2 may indicate a different chain folding behavior from that of solution crystallization. We designate the two regions having the short edge (the *a*-axis) as sectors A and the other two regions involving the long edge (the *b*-axis) as sectors B as shown in Figure 2. Note that the sectorization is observed after the sample was prepared following the conventional procedure (the Pt−C shadowing). No specific decoration was used. As a result, this observation is a clear indication that sectors A and B possess different thicknesses, which leads to the shadows along the boundaries between the sectors and allows them to be seen.

The ED results included in Figures 1 and 2 reveal the lamellar crystal possesses a [00l] zone, and a lateral packing of the unit cell III with a = 1.450 nm and b = 1.120 nm, which agrees with the unit cell proposed by Lovinger and Lotz (the unit cell has c = 0.740 nm).[3−6] This also indicates that the electron beam is parallel to the chain direction and therefore, the *c*-axis is perpendicular to the substrate. Furthermore, it has also been indicated by Lotz and Lovinger and Lovinger *et al.*[3−6] that at the high temperatures (above 125 °C in this case), sharp reflections can be indexed as a pure cell III lattice having the space group *Ibca*, Finally, there is no difference in unit cell orientation observed from the ED patterns in the different sectors, indicating that the lamellar crystal shown in Figure 2 is a regular single crystal.

With increasing molecular weight, growth of sectorized lamellar single crystals becomes increasingly difficult. However, highly faceted, regular, lath-shaped nonsectorized lamellar single crystals can also be observed even when the molecular weight is as high as M_n = 132 000 as shown in Figure 3. The ED pattern from this s-PP fraction is the same as those shown in Figures 1 and 2.

Along the *c*-direction, the lamellar thickness observed by TEM experiments is defined to be a summation of one crystal stem layer and two amorphous layers on the top and bottom of the lamellar crystal. Figure 4 shows an AFM micrograph (top view) of an s-PP single crystal grown at 125 °C, and Figure 5 is a sectorized lamellar single crystal grown at 130 °C. The AFM image provides the same information about the single-crystal morphology as that obtained from TEM observations. Quantitative measurements of the lamellar thickness via the line scanning function of AFM in the s-PP lamellar single crystals formed at 125 °C yield values between 25 and 30 nm and the thickness seems to be uniform across the top surface of the lamellar crystal. For the sectorized lamellar single crystals, on the other hand, a drastic difference in the lamellar thickness is found for the two different sectors. The B sector (having the long edge along the *b*-axis) is thicker than the A sector (having the short edge along the *a*-axis) by a ratio of 3 to 2 (approximately 30 to 20 nm). Note that we have made the plausible assumption that the bottom surface of the A sector lies on the substrate.

Although a minor thickness difference between two sectors (surface domains) may be found in a polymer lamellar single crystal, such as in the case of PE single crystals grown from solution,[18] it is difficult to explain the observations shown in Figures 2 and 5. Several questions may be raised. First, is the thickness difference truly a representation of the difference in lamellar crystal thickness? If it is, the crystal growth has to be anisotropic along the 100 and 010 directions, and two different nucleation barriers with different thicknesses are expected. Second, if the crystal stem thicknesses of the A and B sectors are similar, the amorphous layer in the B sector must be thicker to make it thicker than the A sector. Is this associated with different chain folding conformations? Third, why can this difference be observed only at high crystallization temperature and relatively low molecular weight (in this case, at 130 °C and M_n = 33 300)? Some of these questions may be answered in the study of chain folding behavior in these lamellar single crystals. Others are the focus of our ongoing research.

Polyethylene Decoration on the Lamellar Single Crystals. The chain folding direction can traditionally be studied in two ways. One is the polymer decoration method based on the vaporization and condensation−crystallization of PE upon the fold surface of the polymer, which was first reported by Wittmann and Lotz in the early 1980s.[14,15] The PE molecular fragments are then aligned and crystallized on the fold surface to form rodlike crystals. The orientation of these rod crystals is therefore perpendicular to the chain fold direction of the lamellar single crystal. Figure 6 shows one example of our extensive efforts to obtain reasonable observations of PE decoration on the surface of a nonsectorized s-PP lamellar single crystal. As shown in this figure, the decorated PE rod crystals possess

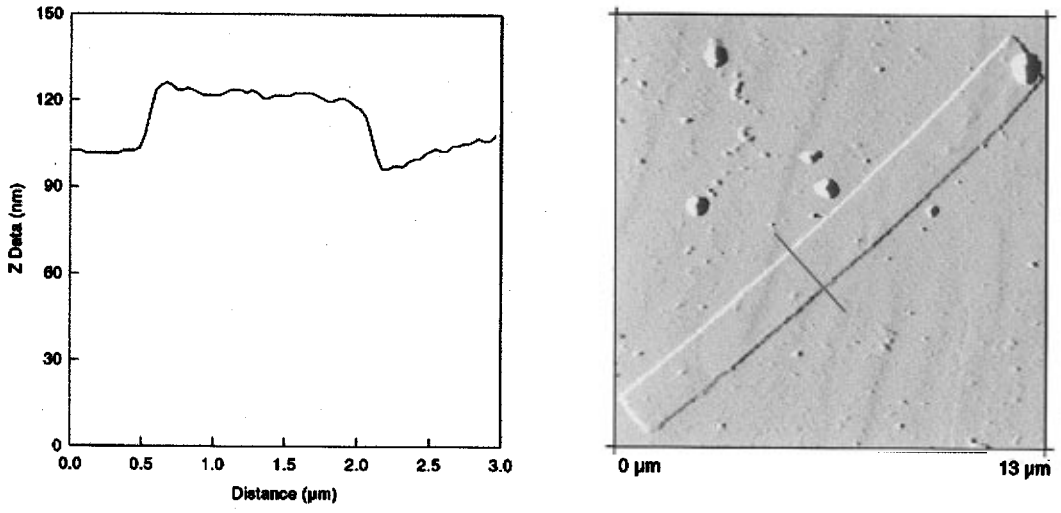

Figure 4. AFM observations of s-PP lamellar single crystals crystallized at 125 °C (M_n = 33.3K).

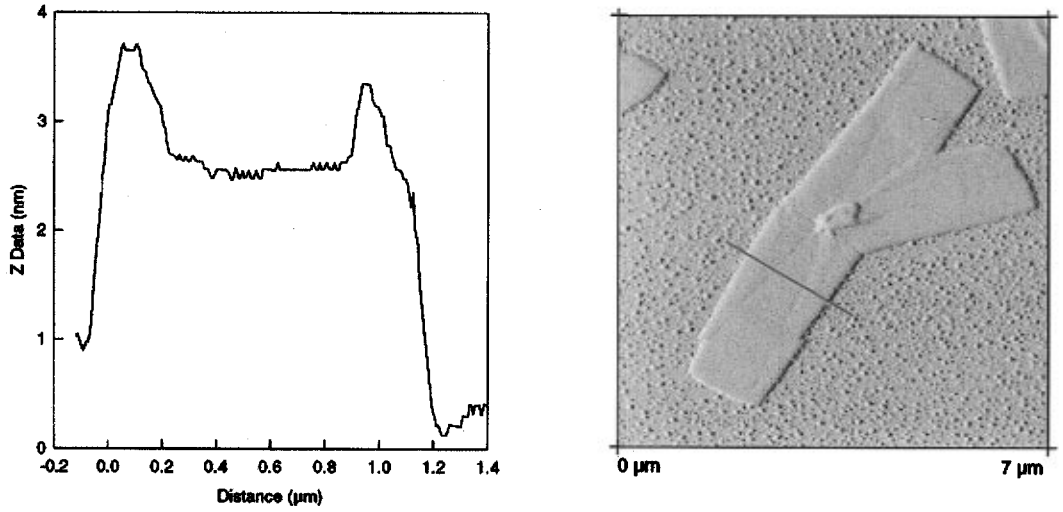

Figure 5. AFM observations of s-PP lamellar single crystals having sectorization crystallized at 130 °C (M_n = 33.3K).

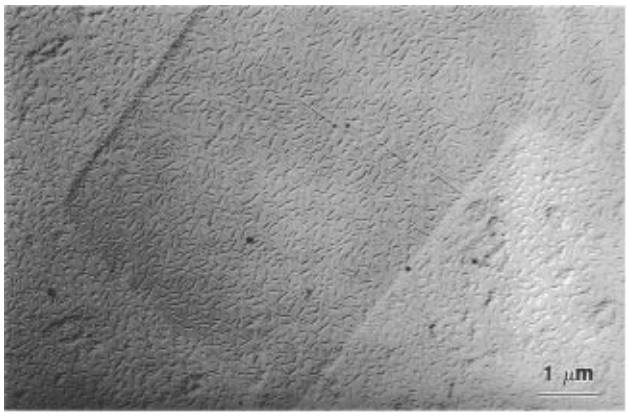

Figure 6. Crystal morphology of PE-decorated s-PP single-crystal surface without sectorization.

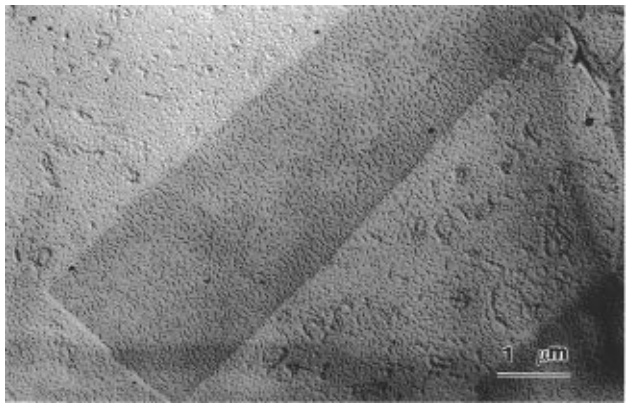

Figure 7. Crystal morphology of PE-decorated s-PP single crystal surface having sectorization.

several aligned directions on the fold surface of the s-PP single crystals. A definite conclusion for the preferred orientational direction of PE rod crystals seems to be difficult to reach.

On the other hand, Figure 7 illustrates PE decoration on the sectorized s-PP lamellar single crystal. The rodlike PE crystals on the top of the lamellar surface in the A sectors again show little evidence of a preferred orientation. In the B sectors, it is clear that along the long edges (the *b*-axis) a majority of the PE rod crystals are aligned more or less perpendicular to the *b*-axis, indicating that the chain folding direction in this sector is along the *b*-axis. This observation is in agreement with the previous report by Lovinger *et al.*[11] and clearly indicates that in the sectors A and B, the chain folding behavior is different.

Several possibilities for the lack of a preferred orientation of PE rod crystals decorated on the s-PP fold crystal surface may be speculated. One of the possibilities may be that the chain folds do not follow a single crystalline plane. Therefore, the fold surface provided

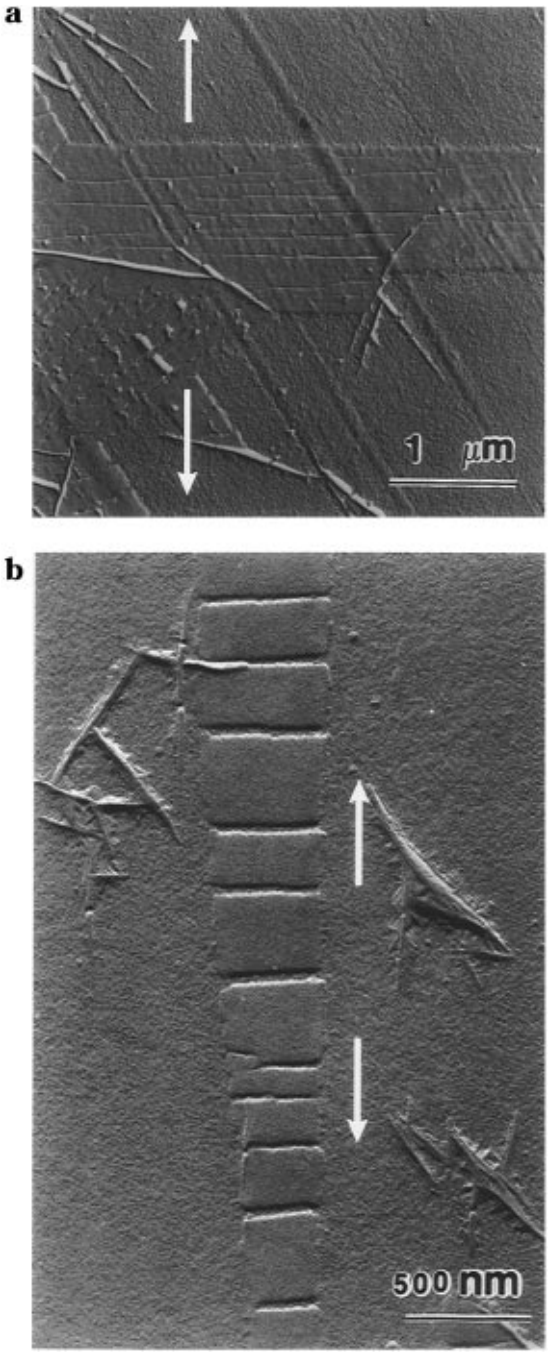

Figure 8. Two s-PP lamellar single crystals (M_n = 33.3K) after deformation along the *a*-axis (a) and along the *b*-axis (b).

for the growth of the PE rod crystals is not macroscopically large enough to allow the construction of a uniformed orientation for the rod crystals. For example, if the chain folding is assumed to have two possibilities which are along both the 110 and $\bar{1}10$ directions, a random distribution of these two possibilities may significantly disturb the orientation in the growth of the PE rod crystal (see below). Another possibility which could affect the rod crystal orientation may be the folded chain conformations. If the s-PP molecules in the A sectors do not possess tight chain folds and the amorphous layer on the top of the crystal stems is rather irregular, this may obscure the alignment and growth of the PE rod crystals. In the sectorized lamellar single-crystal surfaces, the PE decoration may also be affected by the thickness difference between the two sectors.

Single-Crystal Deformation. To further understand the chain folding direction in s-PP single crystals, a second method, single-crystal deformation, has also been carried out. By elongating the thin-film substrate, the single crystals may be broken apart along a certain crystallographic plane to form microcracks which are related to the elongation direction. The deformed crystals may be examined under TEM to observe the appearance of a microfibrillar texture in the cracks to determine the chain folding direction in the single crystals.[16,17] This requires that the polymers examined possess a relatively high degree of polymerization in order to keep continuity of the regular folding direction in the crystal. Then, the molecules may be pulled out to form microfibrils during deformation. Micrographs a and b of Figure 8 exhibit morphology after deformation of the lamellar single crystals having a M_n = 33 300. In these micrographs, deformation directions along both the *a*- and *b*-axes can be seen and multiple cracks are found in both cases. Nevertheless, no obvious microfibrils can be found in the cracks. This indicates that for a lamellar crystal, the constituent chains must have enough chain continuity to form microfibrils. In other words, the molecular weight of the s-PP has to be relatively high. As a result, an s-PP fraction with M_n = 132 000 was chosen to grow single crystals for the deformation method. However, a downside to this choice is that we may have fewer opportunities to study the chain folding behavior in microsectorized lamellar crystals.

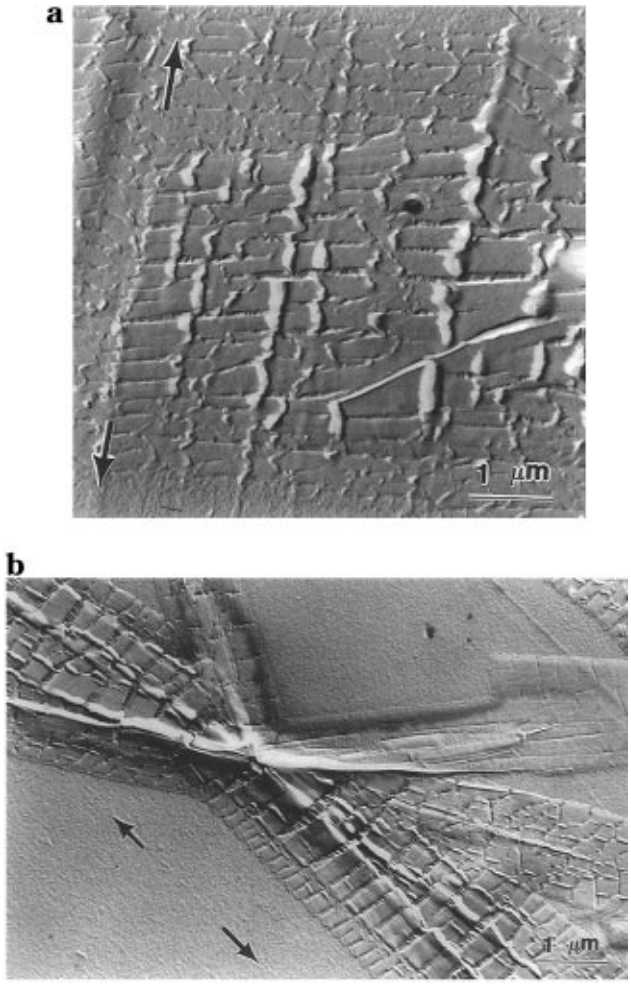

Figure 9. Lamellar single crystals having M_n = 132.0K after deformation along both the *a*- (a) and the *b*-axes (b).

Micrographs a and b of Figure 9 show the deformation along both the *a*- and *b*-axes of the s-PP lamellar single crystals having M_n = 132 000. Microfibrils can be

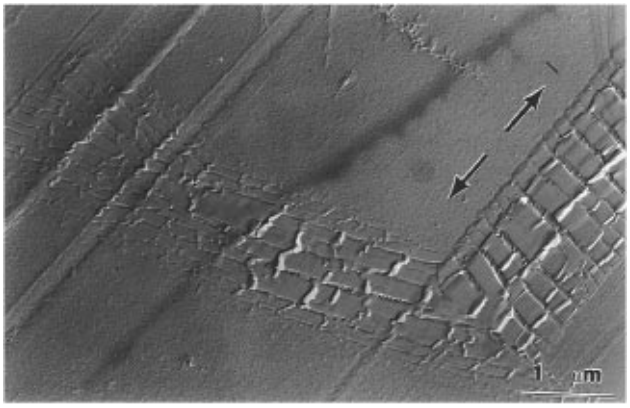

Figure 10. Two lamellar single crystals having $M_n = 132.0$K after deformation along both the *a*- and the *b*-axes.

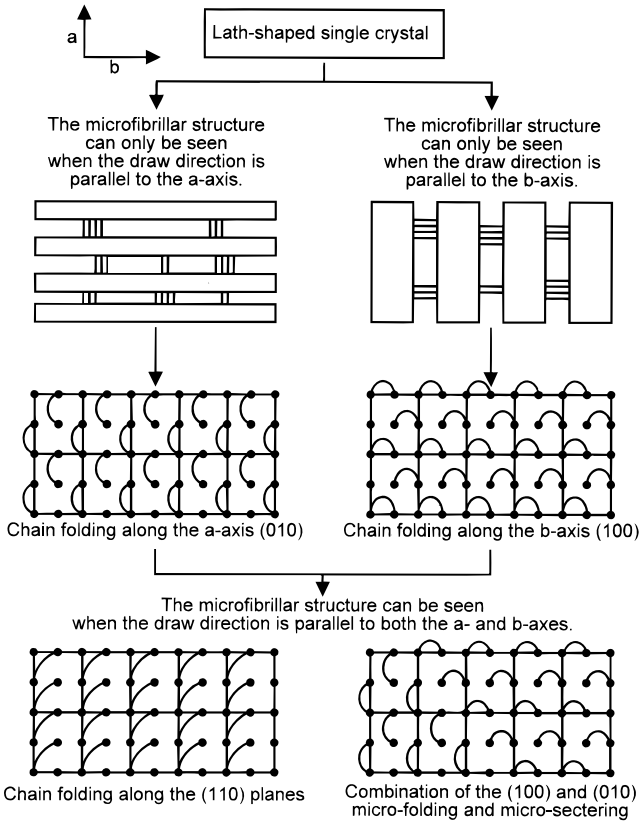

Figure 11. Schematic of chain folding in s-PP lamellar single crystals based on single-crystal deformation experiments.

observed across some of the cracks and they are parallel to the deformation directions. It is evident that some chain molecules are unfolded and pulled out from their original crystals and recrystallized to form the microfibrillar structure. In Figure 9a, perpendicular to the cracks, some overlapped crystals can also be observed which were possibly formed during the deformation along the *a*-axis since the crystal must be compressed along the *b*-axis at the same time. Furthermore, these overlapped crystals sometimes give rise to orientation along the (110) planes (see below). In Figure 10, two single crystals are connected and the deformation direction is almost parallel to the *a*-axis of one crystal and the *b*-axis of the other. Microfibrils exist in the cracks of both crystals and again, the fibrillar direction is parallel to the corresponding deformation direction.

All of these observations may be presented in a schematic as shown in Figure 11. If the chain folding direction is completely along the *b*-axis, the cracks

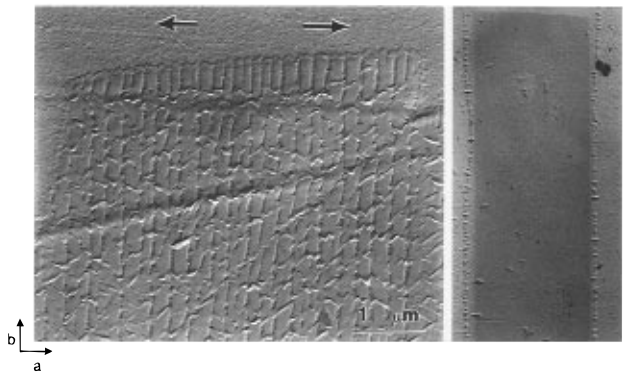

Figure 12. Tip and edge morphology of the s-PP single crystals after deformation along the *a*-axis.

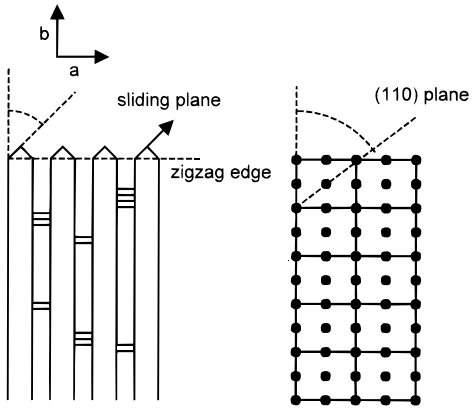

Figure 13. Schematic illustration of the edge formation along the (110) planes.

formed during the deformation along the *a*-axis should exhibit clean edges and no microfibrillar structure should be observed since no chain connectivity due to the chain folding exists along the *a*-axis. On the other hand, if the chain folding direction is completely along the *a*-axis, the cracks along the *b*-axis should not show any microfibrillar crystals. Two possibilities may be proposed to explain the observation in Figure 10: chain folding along the (110) planes or a combination of the (100) and (010) microfolding and microsectoring.

Additional evidence to support the chain folding models may be found from the edge morphology of the single crystals after deformation along the *a*-axis. Figure 12 shows that the edges of the crystal along the *a*-axis possess a zigzag shape with an angle of roughly $\pm 52°$. In other words, between two neighboring cracks, the lamellar fragments which originally follow the flat edge along the *a*-axis (also included in Figure 12 as a reference) become tiplike, and two sliding planes are obvious. After careful measurements of the angles, the sliding planes can be identified as the (110) planes. A schematic is shown in Figure 13. The zigzag edge morphology is the result of the single crystal deformation. Chain molecules are pulled out from the crystal and slide along a certain crystallographic plane at the edges. The formation of this sliding plane can only follow the chain continuity, namely, the chain folding direction. Since the sliding planes have been shown to be the (110) planes, it can be concluded that either the folding direction is along the (110) planes or the (100) and (010) microsectors are aligned along the (110) planes.

Conclusion

In summary, we have found two different types of highly faceted, regular, lath-shaped s-PP lamellar single crystals: nonsectorized and sectorized crystals, depending on crystallization temperature and molecular weight. The two sectors (A and B sectors) in the sectorized single crystals show different thicknesses and the thickness ratio is 3 to 2 for the B sectors which have the long edge (along the *b*-axis) with respect to the A sectors (which have the short edge along the *a*-axis). The observations of PE decoration on the fold surface of s-PP single crystals indicate that little preferred orientation of the PE rod crystals can be found on the nonsectorized single crystals. For sectorized single crystals, the fold direction is along the (010) planes in the B sectors and again, little preferred orientation can be found in the A sectors. In the single-crystal deformation method, only nonsectorized single crystals can be investigated due to the high molecular weight requirement. A microfibrillar structure can be found along both the *a*- and *b*-axes, indicating the fold direction may be either along the (110) planes or a combination of the (100) and (010) microfolding and microsectoring. The zigzag edges on the lamellar fragments after deformation along the *a*-axis can be observed and the chain molecules are pulled out and moved along their 110 fold direction. These morphological observations may serve as initial points to discuss the crystal growth mechanism in s-PP lamellar single crystals.

Acknowledgment. This work was supported by S.Z.D.C.'s Presidential Young Investigator Award from the National Science Foundation (DMR-9157738) and a Scholarship provided by Phillips Petroleum Co.

References and Notes

(1) Natta, G.; Pasquon, I.; Corradini, P.; Perdldo, M.; Pegoraro, M.; Zambelli, A. *Rend. Accad. Naz. Lincei* **1960**, *28*, 541.
(2) Corradini, P.; Natta, G.; Ganis, P.; Temussi, P. *J. Polym. Sci., Part C* **1967**, *16*, 2477.
(3) Lotz, B.; Lovinger, A. J.; Cais, R. E. *Macromolecules* **1988**, *21*, 2375.
(4) Lovinger, A. J.; Lotz, B.; Davis, D. D. *Polymer* **1990**, *31*, 2253.
(5) Lovinger, A. J.; Davis, D. D.; Lotz, B. *Macromolecules* **1991**, *24*, 552.
(6) Lovinger, A. J.; Lotz, B.; Davis, D. D.; Padden, F. J., Jr. *Macromolecules* **1993**, *26*, 3494.
(7) De Rosa, C.; Corradini, P. *Macromolecules* **1993**, *26*, 5711.
(8) Chatani, Y.; Maruyama, H.; Noguchi, K.; Asanuma, T.; Schiomura, T. *J. Polym. Sci., Polym. Lett. Ed.* **1990**, *28*, 393.
(9) Chatani, Y.; Maruyama, H.; Asanuma, T.; Shiomura, T. *J. Polym. Sci., Polym. Phys. Ed.* **1991**, *29*, 1649.
(10) Marchetti, A.; Martuscelli, E. *J. Polym. Sci., Polym. Phys. Ed.* **1974**, *12*, 1649.
(11) Lovinger, A. J.; Lotz, B.; Davis, D. D.; Schumacher, M. *Macromolecules* **1994**, *27*, 6603.
(12) Rodriguez-Arnold, J.; Zhang, A.; Cheng, S. Z. D.; Lovinger, A. J.; Hsieh, E. T.; Chu, P.; Johnson, T. W.; Honnell, K. G.; Geerts, R. G.; Palackal, S. J.; Hawley, G. R.; Welch, B. *Polymer* **1994**, *35*, 1884.
(13) Rodriguez-Arnold, J.; Bu, Z.; Cheng, S. Z. D.; Hsieh, E. T.; Johnson, T. W.; Geerts, R. G.; Palackal, S. J.; Hawley, G. R.; Welch, B. *Polymer* **1994**, *35*, 5194.
(14) Wittmann, J.-C.; Lotz, B. *Makrmol. Chem., Rapid Commun.* **1982**, *3*, 733.
(15) Wittmann, J.-C.; Lotz, B. *J. Polym. Sci., Polym. Phys. Ed.* **1985**, *23*, 205.
(16) Geil, P. H. *Polymer Single Crystals;* Wiley-Interscience: New York, 1963.
(17) Reneker, D. H. *J. Polym. Sci.* **1965**, *A3*, 1069.
(18) Nakagawa, Y.; Hayashi, H.; Takahagi, T.; Soeda, F.; Ishitani, A.; Toda, A.; Miyaji, H. *Jpn. J. Appl. Phys.* **1994**, *33*, 3771.

MA9603793